

LEVERAGING GANS TO IMPROVE CONTINUOUS PATH KEYBOARD INPUT MODELS

Akash Mehra, Jerome R. Bellegarda, Ojas Bapat, Partha Lal, Xin Wang

Apple Inc., Cupertino, California 95014, USA

ABSTRACT

Continuous path keyboard input has higher inherent ambiguity than standard tapping, because the path trace may exhibit not only local overshoots/undershoots (as in tapping) but also, depending on the user, substantial mid-path excursions. Deploying a robust solution thus requires a large amount of high-quality training data, which is difficult to collect/annotate. In this work, we address this challenge by using GANs to augment our training corpus with user-realistic synthetic data. Experiments show that, even though GAN-generated data does not capture all the characteristics of real user data, it still provides a substantial boost in accuracy at a 5:1 GAN-to-real ratio. GANs therefore inject more robustness in the model through greatly increased word coverage and path diversity.

Index Terms— Continuous path recognition, generative adversarial networks, style transfer, embedded devices

1. INTRODUCTION

Entering text on a mobile device involves tapping a sequence of intended keys on a soft keyboard of limited size. Continuous path input, where users keep sliding their finger across the screen until the intended word is complete, offers an alternative input modality [1]. After users gain proficiency with such an option, they often find entering words with one single continuous motion across the keyboard easier and faster [2], [3]. Just like for regular predictive typing, recognition relies on robust pattern matching enhanced with a statistical language model in order to predict the intended word [4].

Existing supervised solutions (e.g., [5]) based on recurrent neural networks (RNNs) call for a large annotated corpus of paths, ideally associated with every token in the supported lexicon. Due to prohibitive collection and annotation costs, however, the size of that training corpus is rarely large enough to achieve the required level of robustness. This observation has prompted a number of investigations into programmatically generating paths that could be used as proxies for real user-generated paths. In [5], for example, the authors generated synthetic paths by connecting the characters within a word using an algorithm that minimizes jerk [6], an approach inspired by human motor control theory (cf., e.g., [7], [8]).

Typically, the parameters of the synthesis algorithm are tuned manually until generated paths look “similar enough” to

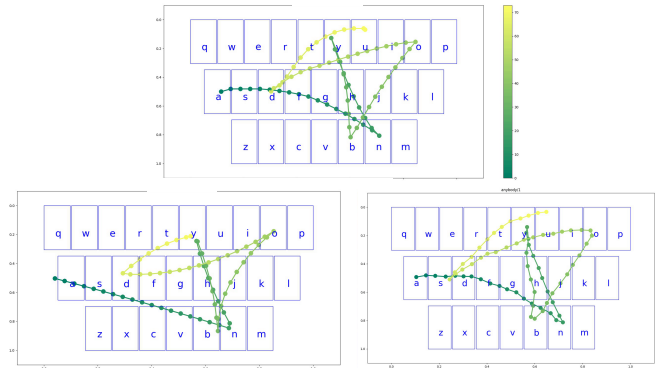


Fig. 1. Path visualization for input word “anybody”—color changes from green to yellow with time. Typical user path (top), programmatically generated synthetic path (bottom left), and GAN-generated synthetic path (bottom right).

real user paths (based on human judgments of a small number of paths [9]). The resulting synthetic paths adequately convey the associated words, and can even incorporate such artifacts as undershooting and overshooting some target keys. However, they are intrinsically restricted in their expressiveness, and do not fully capture the variability of user paths. To illustrate, Fig. 1 shows a typical user path (top) and synthetic path (bottom left) for the word “anybody.”

In this paper, we describe a more flexible approach relying on generative adversarial networks (GANs) [10], [11]. Given an initial synthetic path produced with simple cubic splines [7], we transform it in such a way that it conforms to the kind of user idiosyncrasies observed across the entire set of real user paths available. This problem can be viewed as an instance of style transfer, where the goal is to synthesize a given style of expression while constraining the synthesis to preserve some original content (cf. [12]). The kind of path that results is illustrated at the bottom right of Fig. 1. GAN generation tends to more faithfully render human-like artifacts, resulting in better proxies for real user-generated paths.

The paper is organized as follows. In the next section, we describe the multi-task bidirectional long short-term memory (bi-LSTM) architecture we adopted for continuous path style transfer. In Section 4, we specify the proper objective function to use. In Section 5, we discuss our experimental setup, results observed, and insights gained. Finally, in Section 6 we conclude with a summary and further perspectives.

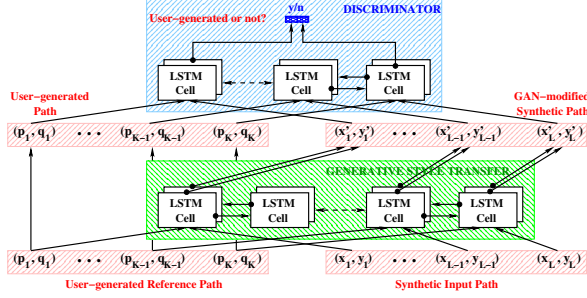


Fig. 2. GAN architecture for path style transfer.

2. STYLE TRANSFER ARCHITECTURE

Style transfer has been an active area of research in computer vision, and there is a large body of work on image style transfer: cf., e.g., [13]–[15]. The basic idea is to bias the generative model in GANs according to the desired style of image [16]. Given the inherent sequential nature of paths, RNNs are more appropriate for path style transfer than the convolutional neural networks used in image style transfer. Hence the architecture illustrated in Fig. 2. Both generative and discriminative models are realized via bi-LSTMs to avoid vanishing gradients [17]. In each case only one LSTM is shown, but in practice it is extended to a deeper network.

In Fig. 2, an initial synthetic input path X (represented by a sequence of sampled points $\{(x_1, y_1) \dots (x_L, y_L)\}$) is transformed into a “more human-like” synthetic path $Y = \{(x'_1, y'_1) \dots (x'_L, y'_L)\}$ on the basis of an available set of user-generated reference paths $P = \{(p_1, q_1) \dots (p_K, q_K)\}$, which are collectively representative of a range of observed user idiosyncrasies (“style”). Both bi-directional LSTMs leverage knowledge of the entire path under consideration: the generative model to suitably shift each point so as to make the whole path more congruent to one generated by a user, and the discriminative model to decide whether the path is user-generated (as in $P = \{(p_1, q_1) \dots (p_K, q_K)\}$) or not (as in $Y = \{(x'_1, y'_1) \dots (x'_L, y'_L)\}$). Fig. 2 promotes the generation of user-realistic paths, because the discriminator will eventually abstract out user behaviors observed in the P paths and thus will tend to force the generator to discard transformations that do not account for such behaviors.

The architecture of Fig. 2 is not completely satisfactory, however, because there is no guarantee that the transformed path will still be associated with the correct input word. It could be, for example, that the original synthetic path becomes virtually indistinguishable from a real user path corresponding to a different word, which would lead to a loss of discriminability between words. This realization caused us to add a path recognition module, resulting in the architecture depicted in Fig. 3. By taking into account the built-in constraints enforced by the classifier, this network is more likely to abstract out, from the broad inventory of paths occurring in the reference corpus, those discriminative elements of user

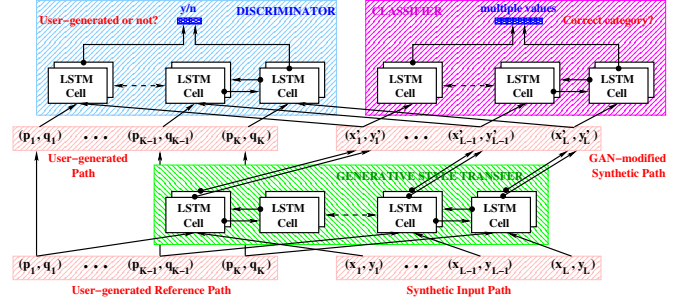


Fig. 3. Multi-task GAN architecture for path generation with joint style transfer and classification.

generated paths that are most relevant to the current word.

Compared to Fig. 2, every transformed path Y generated by the style transfer model is passed not just to the discriminator, but also to a classifier which verifies that the decoded category is indeed still associated with the current word. That way, we entice the generative model to produce a path which is not just similar to a real user path, but also generally congruent with typical paths for the current word as observed in the entire reference corpus. The rest of the system is as in Fig. 2. In particular, the discriminative model still receives an input consisting of either a user-generated path P or a synthetic path Y , which implies a multi-task objective function.

3. MULTI-TASK OBJECTIVE FUNCTION

Generative adversarial transfer operates under the assumption that any path P from the reference corpus is drawn from a true distribution \mathbb{D} representative of all user-generated behaviors observed across the available corpus, and that the transformed path Y generated from the initial input path X by the style transfer model follows a distribution \mathbb{D}' that is “close” to \mathbb{D} according to some suitable closeness metric. The objective of GAN training is therefore for \mathbb{D}' to converge to \mathbb{D} .

Looking back at Fig. 2, the generative model \mathcal{G} transforms the input X into $Y = \mathcal{G}(X)$, taking into account information provided by P so that Y conforms to the style of P . The discriminator \mathcal{D} then estimates the probability that a given path is drawn from \mathbb{D} rather than \mathbb{D}' . Ideally, $\mathcal{D}(P) = 1$ when $P \sim \mathbb{D}$ and $\mathcal{D}(Y) = 0$ when $Y \sim \mathbb{D}'$, with the additional constraint that $Y \approx X$.

This corresponds to a minimax two-player game, in which the generative and discriminative models \mathcal{G} and \mathcal{D} are trained jointly via solving:

$$\begin{aligned} \min_{\mathcal{G}} \max_{\mathcal{D}} \mathcal{K}(\mathcal{D}, \mathcal{G}) &= \mathbb{E}_{P \sim \mathbb{D}} \left\{ \log [\mathcal{D}(P)] \right\} \\ &+ \mathbb{E}_{\mathcal{G}(X) \sim \mathbb{D}'} \left\{ \log [1 - \mathcal{D}(\mathcal{G}(X))] \right\} \\ &+ \mathbb{E}_{\mathcal{G}(X) \sim \mathbb{D}'} \left\{ \Delta [X, \mathcal{G}(X)] \right\}, \quad (1) \end{aligned}$$

where $\mathcal{K}(\mathcal{D}, \mathcal{G})$ denotes the overall cost function, and $\Delta[X, Y]$ is a suitable distance metric which is 0 when $X = Y$, and increases away from 0 as the paths X and Y become more and more dissimilar. Maximizing (1) over \mathcal{D} while minimizing it over \mathcal{G} ensures that \mathcal{G} generates paths that are as maximally similar to X as possible, while looking like they might have been drawn from the true distribution \mathbb{D} of user-generated paths. Assuming that \mathcal{D} and \mathcal{G} comprise a sufficient number of parameters, after enough training iterations, the distribution \mathbb{D}' will converge to \mathbb{D} [10]. In other words, the network \mathcal{G} learns to synthesize a path $Y = \mathcal{G}(X)$ that eventually looks like it was user-generated, but still preserves the main characteristics of the initial path X .

The next step is to properly inject the classifier from Fig. 3. Recognizing the word $w = w_j$ associated with the transformed path Y involves mapping a potentially long sequence of feature vectors to a much shorter sequence of characters. A suitable loss function for this type of sequence classification task is the Connectionist Temporal Classification (CTC) loss [18]. The CTC loss function trains RNNs on unaligned targets through maximizing the sum of probabilities of all step-wise sequences that correspond to the target sequence. Concretely, for a given classifier \mathcal{C} , this loss is given as follows:

$$\mathcal{L}(\mathcal{C}) = -\log \left(\sum_{\pi \in \mathcal{A}(w)} \prod_{k=1}^K o_k^{(\pi)} \right), \quad (2)$$

where w is the target transcription (word), $\mathcal{A}(w)$ is the set of all CTC transcriptions of a target transcription (e.g., for the word “data”, allowable transcriptions may include “daata”, “datta”, “dddata”, etc.), and $o_k^{(\pi)}$ denotes the output of the LSTM at time step k for a particular CTC transcription π of the target transcription of length K characters.

Computing the CTC loss (2) typically involves inserting blanks at the beginning, between symbols, and at the end of the target transcription. The forward-backward algorithm can then be used to extract all possible transcriptions π . The desired output follows after removing blanks and repetitions. Using the CTC loss function during training thus makes it possible to train the network to output characters directly, without the need for an explicit alignment between input and output sequences.

The final step is to combine the two objective functions above to make sure that the optimal generated path is indeed still associated with the current word. In practice, to train the network of Fig. 3, we therefore consider a linear interpolation of the two objective functions:

$$\mathcal{M}(\mathcal{C}, \mathcal{D}, \mathcal{G}) = \lambda \cdot \mathcal{K}(\mathcal{D}, \mathcal{G}) + (1 - \lambda) \cdot \mathcal{L}(\mathcal{C}), \quad (3)$$

where the scalar interpolation coefficient λ is a tunable weighting parameter adjusting the contribution from the main (GAN) and auxiliary (classification) tasks.

After such multi-task adversarial training is complete, the discriminative model has learned to abstract out user idiosyn-

crasies observed in the reference corpus, so the generated path Y ends up taking into account the desired range of user behaviors, while still preserving the main characteristics of the input content X (and ideally behaving in the same way regarding recognition accuracy). Thus, the generative network in Fig. 3 in principle leads to the most realistic rendering of input paths given the reference corpus.

4. EXPERIMENTAL RESULTS

We conducted continuous path recognition experiments using models trained on a variety of corpora. We drew from a set of 2.2M user paths (referred below with the prefix “U”) covering 55K English words collected from a diversity of users in a variety of conditions. Specifically, 665 users (roughly half males, half females) ranging in age from 18 to 70 years produced paths on 6 layouts with various screen sizes. Thus each participant generated 3300 paths on the average. Approximately half of the paths were generated using the thumb finger, with the other half generated with the index finger. In line with [19], the participants were chosen to attain a proportion of left-handed users of about 20%.

We then generated a comparable set of initial synthetic paths obtained via cubic splines [7], referred below with the prefix “S.” Finally, we also used these synthetic paths as initial exemplars for style transfer, using the multi-task GAN style transfer architecture of Fig. 3, where the GAN was trained using 1.1M user paths. This led to the generation of a comparable set of more sophisticated GAN-generated paths, referred below with the prefix “G.” For test data, we collected a corpus of 59,469 user paths covering approximately 25K English words included in the 55K inventory above. To better isolate modeling performance across different training compositions, we measured Top-1 recognition accuracy, and thus deliberately ignored language model rescoring.

The results of our experiments are summarized in Table 1. As baseline, we trained models on 1.1M paths from each set (top 3 rows, labelled **U1**, **S1**, and **G1**). Then we analyzed what happens when doubling (next 3 rows, labelled **U2**, **U1+S1**, and **U1+G1**) and tripling (following 3 rows, labelled **U1+S1+G1**, **U1+G2**, and **U2+G1**) the amount of training data, via folding in either more user paths or more synthetic/GAN paths. Finally, we investigated whether the same trends hold when training on 4.4M paths, only half of which are user paths (following two rows, labeled **U2+S2** and **U2+G2**) and when training on approximately 13M paths, only about 1/6 of which are user paths (last row, labeled **U2+G10**).

The most salient observation is that adding GAN-generated data is much more effective than adding less user-realistic synthetic data. Interestingly, GAN-generated paths by themselves prove no more effective than synthetic paths by themselves (compare **U1** vs. **S1** vs. **G1** in the top 3 rows). This may be traced to a lack of diversity in data generation, or possibly a failure to capture all relevant user artifacts. How-

Table 1. Continuous path recognition results using a variety of training compositions, given an underlying lexicon of 55K English words. The test corpus comprises 59,469 paths covering 24,002 words. No language model is used.

Training Composition (Number of Paths)	Top-1 Acc.
U1 (1.1M user only)	58.5%
S1 (1.1M synt. only)	35.0%
G1 (1.1M GAN only)	33.7%
U2 (2.2M user only)	62.2%
U1+S1 (1.1M user + 1.1M synt.)	57.6%
U1+G1 (1.1M user + 1.1M GAN)	62.4%
U1+S1+G1 (1.1M each of user, synt., GAN)	61.4%
U1+G2 (1.1M user + 2.2M GAN)	63.5%
U2+G1 (2.2M user + 1.1M GAN)	64.5%
U2+S2 (2.2M user + 2.2M synt.)	59.5%
U2+G2 (2.2M user + 2.2M GAN)	65.8%
U2+G10 (2.2M user + 10.8M GAN)	66.8%

ever, when used as a complement to user data (compare **U2** vs. **U1+S1** vs. **U1+G1** in the next 3 rows), GAN data clearly outperforms synthetic data—essentially providing the equivalent of training on user data only in terms of accuracy.

This trend is confirmed when folding in more data (compare **U1+S1+G1** vs. **U1+G2** vs. **U2+G1** in the next 3 rows): synthetic data completely fails to help over the (1.1M+1.1M) user/GAN training scenario, while folding in either more user or more GAN data substantially improves the outcome. Note that user data seems to retain its expected edge, as the (2.2M+1.1M) configuration still outperforms the (1.1M+2.2M) configuration by 1% absolute. Again, this may be due to the inherent difficulty of capturing rarely observed user artifacts using a GAN framework. Finally, even better results are obtained in the (2.2M+2.2M) user/GAN configuration, which provides a 3.6% absolute accuracy boost over the baseline 2.2M user training, and the best results are obtained when folding even more GAN data: in the (2.2M+10.8M) user/GAN configuration, we reach a 4.6% absolute boost in accuracy, showing that it is possible to exploit to good effect many multiples of the user-generated data available.

Fig. 4 displays the associated learning curve, i.e., how the error scales with data size. The “steepness” of that learning curve (on a log-log plot) conveys how quickly a model can learn from adding more training samples [20]. For a given model architecture, it also implicitly reflects the quality of the added samples. Given that the green (GAN) slope is slightly less steep than the blue (user) slope, it appears that adding GAN-generated data is somewhat less effective than adding real user data. In other words, GAN-generated data only cap-

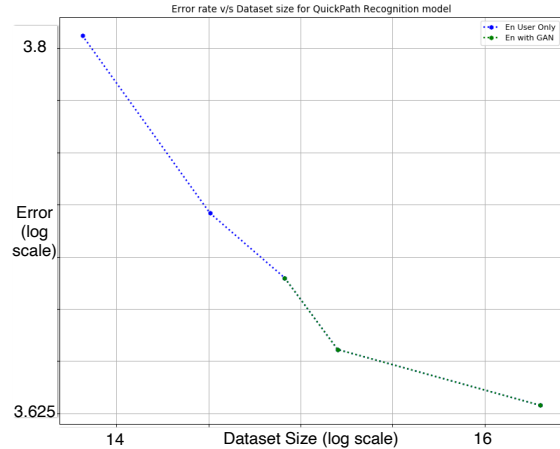


Fig. 4. Log-log plot of continuous path recognition learning curve derived from Table 1. Blue: user data only, green: GAN augmentation.

tures *some* of the desired user characteristics. Still, the learning curve of Fig. 4 bodes well for reducing data collection costs when extending to other languages and scripts.

5. CONCLUSION

In this paper, we have leveraged GANs to synthesize user-realistic training data for learning continuous path recognition models. This approach obviates the need to learn the parameters of a dedicated human motor control model, or to assess the similarity between a synthetic and user-generated path. Such assessment becomes an emergent property of the modeling, which in turn enables practical deployment at scale.

The proposed approach relies on a multi-task adversarial architecture designed to simultaneously carry out two different sub-tasks: (i) generate a synthetic path that generally conforms to user idiosyncrasies observed across reference user-generated paths; and (ii) verify that recognition accuracy for this synthetic path is not negatively impacted in the process. After multi-task adversarial training is complete, the GAN-generated paths reflect a range of realistic user behaviors while still being aligned with the target word.

The generated paths are then folded into the continuous path training corpus, which advantageously increases both word coverage and path diversity. That way, we emulate the acquisition of many more paths from many more users and thereby support training of a more robust model. This solution considerably reduces the collection and annotation costs typically associated with the large corpus of paths required (cf., e.g., [5]). A further improvement will be to streamline the two sequential processes involved: path generation in order to augment the training corpus, followed by standard training of the path recognition model. In principle, the fact that the path generation process already comprises a recognition module could enable consolidation into a unified training performed in end-to-end fashion.

6. REFERENCES

- [1] S. Zhai and P.-O. Kristensson, "The Word-Gesture Keyboard: Reimagining Keyboard Interaction," in *Communications of the ACM*, Vol. 55, No. 9, pp. 91–101, 2012.
- [2] S. Zhai and P.-O. Kristensson, "Shorthand Writing on Stylus Keyboard," in *Proc. ACM Conf. Special Interest Group on Computer-Human Interaction*, pp. 97–104, 2003.
- [3] S. Reyal, S. Zhai, and P.-O. Kristensson, "Performance and User Experience of Touchscreen and Gesture Keyboards in a Lab Setting and in the Wild," in *Proc. 33rd Ann. ACM Conf. on Human Factors in Computing Systems*, pp. 679–688, 2015.
- [4] S. Mitra and T. Acharya, "Gesture Recognition: A Survey," *IEEE Trans. Systems, Man, and Cybernetics*, Part C: Applications and Reviews, Vol. 37, No. 3, pp. 311–324, 2007.
- [5] O. Alsharif, T. Ouyang, F. Beaufays, S. Zhai, T. Breuel, and J. Schalkwyk, "Long Short Term Memory Neural Network for Keyboard Gesture Decoding," in *Proc. Int. Conf. Acoustics, Speech, Signal Processing*, Brisbane, Australia, Sept. 2015.
- [6] P. Quinn and S. Zhai, "Modeling Gesture-Typing Movements," *Human-Computer Interaction*, pp. 1–47, 2016.
- [7] T. Flash and N. Hogan, "The Coordination of Arm Movements: An Experimentally Confirmed Mathematical Model," in *J. Neuroscience*, Vol. 5, pp. 1688–1703, 1985.
- [8] J. Müller, A. Oulasvirta, and R. Murray-Smith, "Control Theoretic Models of Pointing," *ACM Trans. Computer-Human Interaction*, Vol. 24, No. 4, Aug. 2017.
- [9] S. Zhai, J. Kong, and X. Ren, "Speed-Accuracy Tradeoff in Fitts' Law Tasks on the Equivalency of Actual and Nominal Pointing Precision," *Int. J. Human-Computer Studies*, Vol. 61, No. 6, pp. 823–856, 2004.
- [10] I. Goodfellow, J. Pouget-Abadie, M. Mirza, B. Xu, D. Warde-Farley, S. Ozair, A. Courville, and Y. Bengio, "Generative Adversarial Nets," in *Proc. Neural Information Processing Systems*, Dec. 2014.
- [11] T. Salimans, I. Goodfellow, W. Zaremba, V. Cheung, A. Radford, and X. Chen, "Improved Techniques for Training GANs," *arXiv:1606.03498v1*, Jun. 2016.
- [12] A. Shrivastava, T. Pfister, O. Tuzel, J. Susskind, W. Wang, and R. Webb, "Learning from Simulated and Unsupervised Images through Adversarial Training," in *Proc. Conf. Computer Vision and Pattern Recognition*, pp. 2107–2116, 2017.
- [13] L.A. Gatys, A.S. Ecker, and M. Bethge, "A Neural Algorithm of Artistic Style," *arXiv:1508.06576v2*, Sept. 2015.
- [14] J. Johnson, A. Alahi, and F.F. Li, "Perceptual Losses for Real-Time Style Transfer and Super-Resolution," *arXiv:1603.08155v1*, Mar. 2016.
- [15] P. Isola, J.-Y. Zhu, T. Zhou, and A. Efros, "Image-to-Image Translation with Conditional Adversarial Nets," in *Proc. Conf. Computer Vision and Pattern Recognition*, 2017.
- [16] L.A. Gatys, A.S. Ecker, and M. Bethge, "Image Style Transfer Using Convolutional Neural Networks," in *Proc. Conf. Computer Vision and Pattern Recognition*, pp. 2414–2423, 2016.
- [17] M. Sundermeyer, R. Schlüter, and H. Ney, "LSTM Neural Networks for Language Modeling," in *Proc. InterSpeech*, pp. 194–197, Sept. 2012.
- [18] A. Graves, S. Fernandez, F. Gomez, and J. Schmidhuber, "Connectionist Temporal Classification: Labelling Unsegmented Sequence Data with Recurrent Neural Networks," in *Proc. ACM Int. Conf. Machine Learning*, pp. 369–376, 2006.
- [19] S. Azenkot and S. Zhai, "Touch Behavior with Different Postures on Soft Smartphone Keyboards," in *Proc. 14th ACM Int. Conf. Human-Computer Interaction with Mobile Devices and Services*, pp. 251–260, 2012.
- [20] J. Hestness, S. Narang, N. Ardalani, G. Diamos, H. Jun, H. Kianinejad, M.M.A. Patwary, Y. Yang, and Y. Zhou, "Deep Learning Scaling is Predictable, Empirically," *arXiv:1712.00409v1*, Dec. 2017.